energies

MDPI

Article

Measurement of Sub-23 nm Particles Emitted from PFI/DI SI Engine Fueled with Oxygenated Fuels: A Comparison between Conventional and Novel Methodologies

Francesco Catapano, Silvana Di Iorio, Agnese Magno *, Paolo Sementa and Bianca Maria Vaglieco

Institute of Science and Technology for Sustainable Energy and Mobility (STEMS)—CNR, Via G. Marconi 4, 80125 Naples, Italy; francesco.catapano@stems.cnr.it (F.C.); silvana.diiorio@stems.cnr.it (S.D.I.); paolo.sementa@stems.cnr.it (P.S.); biancamaria.vaglieco@stems.cnr.it (B.M.V.)

* Correspondence: agnese.magno@stems.cnr.it; Tel.: +39-0817-177-118

Abstract: This study focuses on the measurement of sub-23 nm particles emitted from a small DI/PFI spark ignition engine through conventional techniques and innovative systems. Measurements were performed with well-known systems, such as the EEPS coupled to a PMP-compliant sample conditioning device. Moreover, a novel instrument developed within the European project Sureal-23, the advanced HM-DMA, capable of operating with a simplified conditioning setup was used. The engine was fueled with ethanol, both pure and in blend at 30% v/v. The effects of fuel on the particle emissions were analyzed at different operating conditions. The results highlighted that a larger fraction of emissions consists of particles smaller than 23 nm, and their number changes according to the fuel, injection strategy and operating condition. A significant effect of the sampling system conditions was observed reveling the inception of nucleation mode particles or the condensation of the volatiles onto existing particles depending on the combination fuel/injection strategy. Different trends were noted at certain operating conditions between the results from the EEPS and the advanced HM-DMA ascribable to the different measurement principle and to the dilution system.

Keywords: sub-23 nm particles; spark ignition engine; ethanol; advanced HM-DMA

Citation: Catapano, F.; Di Iorio, S.; Magno, A.; Sementa, P.; Vaglieco, B.M. Measurement of Sub-23 nm Particles Emitted from PFI/DI SI Engine Fueled with Oxygenated Fuels: A Comparison between Conventional and Novel Methodologies. *Energies* **2022**, *15*, 2021. https://doi.org/10.3390/en15062021

Academic Editors: Alessandro Mingotti, Federico Tramarin and Dimitrios C. Rakopoulos

Received: 20 December 2021
Accepted: 8 March 2022
Published: 10 March 2022

1. Introduction

The growing concerns regarding climate change, the deterioration of local air quality and high fuel prices have led to a growing proliferation of electric and fuel-cell vehicles in the market. For the consumer, electrical energy is cheaper than liquid fuel even if there is no certainty that this trend will remain the same in the next year. Moreover, the ecological impact of electrification over the entire life-cycle analysis should be considered [1]. Therefore, it is plausible that internal combustion engines (ICE) will play a dominant role in the powertrain vehicles for the next years [2] even if they represent the main emitter of ultrafine particles in congested urban areas.

In particular, gasoline direct injection (DI) engines emit higher particle numbers (PN) compared to compression ignition engines (CI) equipped with diesel particulate filters (DPF) [3]. In a recent study, Kontses et al. [4] observed that gasoline PFI engines can also have high PN emissions expressing the need of further investigation to accurately evaluate their emission levels and, eventually, the necessity to be regulated.

In this transition period, several solutions are being considered to make SI engines more environmentally friendly. One of these is represented by the renewable fuels, such as oxygenated and synthetic fuels. Ethanol is the most used alternative fuel for SI engines, and it can be used both pure and blended. Due to its clean-burning characteristics and its potential to reduce greenhouse gas emissions [5], its use for vehicle transport is worthy of continuing research studies.

A large fraction of the total number of particles emitted by SI engines, fueled both with fossil fuels and oxygenated fuels, are smaller than 23 nm [6–9], which is the current threshold adopted by the European Union to regulate these emissions [10,11]. The methodology for the emission standards is based on the recommendations of the Particle Measurement Programme (PMP) entailing a first hot dilution at 150 °C, followed by an evaporation tube at 350 °C to remove semi-volatiles and then a Condensation Particle Counter (CPC) with 50% detection efficiency at 23 nm (d50% = 23 nm) [12].

During this process, re-condensation on soot particles or re-nucleation of volatiles can occur. The nucleated particles unlikely grow over 23 nm, thus, the cut-off at 23 nm avoid to take into account the volatile species that can survive the conditioning unit [13]. Zheng et al. [14] provided a study on the nature of sub-23 nm particles downstream of the PMP system on both standard driving cycles and on-road conditions. They hypothesized that most of the sub-11 nm particles were formed from the re-nucleation of vaporized semi-volatiles particles in the evaporation tube (ET) and were not truly solid since sub-11 nm particles reduce drastically at an elevated PMP dilution ratio.

In another study [15], they observed that solid particles in the range of 3 to 10 nm can be formed in the ET from a mixture of semi-volatile hydrocarbons and sulfuric acid particles. They concluded that the PMP protocol works fine with a cut-off diameter of 23 nm. Several studies demonstrated that the emissions of sub-23 nm particles can be more harmful to human health than bigger particles [16,17] indicating the need of their regulation.

To face the challenge of extending the limit on particle emissions down to 10 nm, the Sureal-23 project was funded by Horizon 2020 European Union program with the aim to improve the knowledge on the nature of sub-23 nm particles thus developing new methodologies and techniques for their measure [18]. In this context, the advanced Half Mini Differential Mobility Analyser (HM-DMA) was proposed [19]. This instrument, first developed at Yale University [20] and then improved by SEADM [21], is capable of classifying the particle emissions in the mobility size range 5–30 nm. Its unique feature to operate at high temperature allows to reduce or even eliminate the sample conditioning, thus, avoiding artefact formation and resulting in a more reliable solid particle measurement [22].

The present research study was performed within the European project Sureal-23 with the aim to evaluate the measurement techniques for sub-23 nm particles and analyze the impact of the ethanol, both pure and in blend, on their emissions. The investigation was performed on a small displacement spark ignition (SI) engine equipped with both DI and PFI systems. Tests were performed with gasoline, ethanol and a blend of 30% v/v of ethanol in gasoline (E30). The operating conditions at full load and 2000 and 4000 rpm were investigated as representative of real driving conditions.

Particle measurements in the range from 5.6 to 560 nm were performed through a well-consolidated procedure involving the Engine Exhaust Particle Sizer (EEPS) from TSI (Dumfries, UK) coupled to the Dekati® (Kangasala, Finland) Engine Exhaust Diluter (DEED)—a PMP-compliant conditioning system. To highlight the effect of sampling temperature on the particle size distribution (PSD), with particular focus to the sub-23 nm particles, measurements were also done at temperature of dilution stages in the DEED lowered with respect to the ones prescribed by the PMP protocol. A new system for the characterization of sub-23 nm particles, the advanced HM-DMA was used to measure the particles in the size range from 1 up to 30 nm. In this case, the exhaust gas was sampled by a Dekati® (Kangasala, Finland) single diluter (SD).

2. Methods

2.1. Experimental Apparatus

2.1.1. Test Engine

The experimental setup consisted of the engine system loaded by an electrical dynamometer allowing to maintain the engine speed constant, the operating system and the data acquisition system. The test engine is a four stroke, single cylinder SI engine whose

detailed specifications are reported in Table 1. The engine has a prototype cylinder head of a naturally aspirated DI engine with a displacement of 250 cc. The engine head has four valves and a spark plug mounted in the center. A prototype six-hole injector was installed inside the cylinder between the intake valves. The engine was modified to also operate in PFI configuration with a low pressure three-hole commercial injector installed in the intake manifold.

Table 1. Engine specifications.

Engine	Spark Ignition	
Number of Cylinders	1	
Bore [mm]	72	
Stroke [mm]	60	
Displacement [cm^3]	250	
Compression Ratio	11.5	
Max. Power [kW]	16 @ 8000 rpm	
Max. Torque [Nm]	20 @ 5500 rpm	
Intake	Naturally Aspirated	
Injection system	DI Prototype	PFI commercial
Number of Nozzle Holes	6	3
p_{inj} [bar]	100	3

A schematic of engine head is shown in Figure 1. The excess air ratio (λ) value was measured by a linear lambda sensor Bosch LSU 4.9 mounted at the exhaust. The in-cylinder pressure was monitored through a quartz pressure transducer flush-mounted in the area between the intake and exhaust valves. The operating system included a programmable electronic control unit (PECU) allowing management of the injection and ignition timing. The data acquisition system recorded the in-cylinder pressure, the engine parameters and the exhaust emissions during the tests.

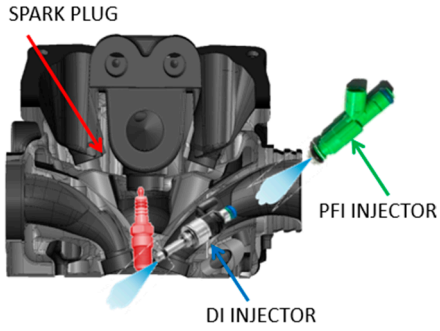

Figure 1. Engine head.

2.1.2. Particle Measurement Systems

The EEPS 3090 from TSI was used to measure real time PSDs. The instrument is capable of measuring, with high accuracy [23], particles in the range from 5.6 to 560 nm in electrical mobility diameter at rate of 10 Hz without discrimination in their nature, whether they are solid or volatile. The EEPS is characterized by a sizing resolution of 16 channels per decade corresponding to 32 channels. Measurements are based on charging the particles applying an electric field and detecting their current at the electrometers where they deposit.

The current is then converted in PSD using a fractal (soot) inversion algorithm taking into account that the engine exhaust particles, specifically carbonaceous agglomerates, differ from spherical particles because agglomerates take up more charge than spheres at a given mobility diameter [24]. Before entering the EEPS, the exhaust gas sample was taken by a 1.5 m long line heated at 150 °C to prevent condensation of combustion water.

The sample was diluted by means of the Dekati® DEED, a PMP-compliant conditioning system. Nucleation particle detection was performed through an advanced HM-DMA characterized by high resolution in the size range 5–30 nm [25] and fast response time down to 1 s [26]. The instrument is a prototype that was developed within the European project Sureal-23. Regarding its working principle, the hot aerosol is charged through Secondary Electrospray Ionisation (SESI), and the particles are classified due to the combination of a well-controlled axial sheath flow and a radial electric field so that only the particles with a well-defined electrical mobility are sent to the DMA outlet [21].

Then, the selected ionized particles are measured by a fast electrometer coupled with the DMA developed by Fernadez de la Mora et al. [26]. The SESI charger is a novel device for the hot aerosol charging, and a global charging efficiency relation has not been well defined yet. In this regard, due to the correlation between the SESI charging efficiency with the concentration of the particles in the sample, the probability density function of the particle size distribution was not calculated, and the size distributions are shown in terms of the ion concentration [27]. The results obtained through the advanced HM-DMA are valuable for a comparison among fuels and engine conditions without the impact of the conditioning system.

The main feature of the Advanced HM-DMA is its capability to work with high aerosol temperature, up to 200 °C due to the presence of heat-tolerant materials for insulating and semiconducting parts [28]. The high operation temperature allows to reduce the exhaust sample conditioning, thus, preventing artifacts from condensable species.

The hot operation mode accuracy of the instrument was tested with reference aerosols against state-of-the-art instruments as shown in [18]. An excellent agreement between the two measurements was observed confirming the reliability of the Advanced HM-DMA hot operation mode and revealing the possibility of using a simplified conditioning setup for solid nucleation-mode particle measurement.

In this research study, a low dilution ratio was applied to the exhaust gas sample before entering the advanced HM-DMA. The particle counter was installed downstream from a Dekati® SD characterized by a dilution ratio of 1:10 and a dilution temperature of 150 °C. Even in this case, the exhaust gas sample was taken by a 1.5 m long line heated at 150 °C to avoid water condensation.

For both configurations, the transport lines, diluters, evaporation tubes and other components were properly developed to reduce the particle losses. A schematic of the configurations used for the particle number measurement is shown in Figure 2.

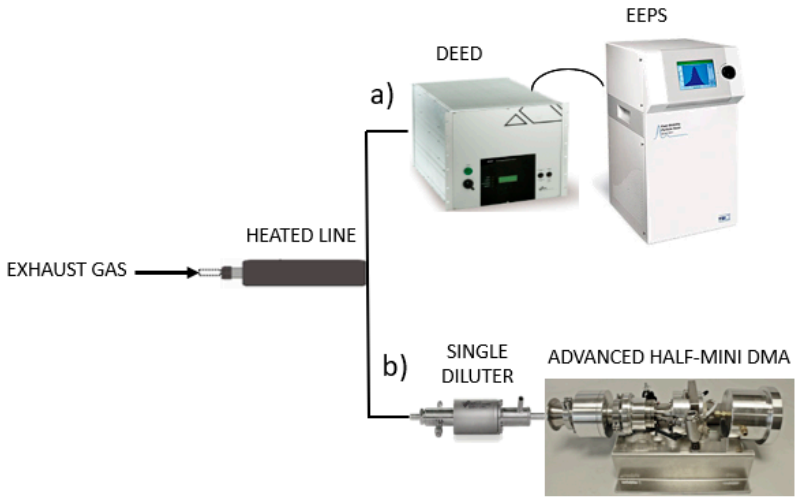

Figure 2. Instruments for particle number measurement: (**a**) EEPS coupled to the DEED. (**b**) Advanced HM-DMA connected to the SD.

2.2. Experimental Conditions

Experiments were performed in steady state conditions at two engine speeds, 2000 and 4000 rpm, with wide open throttle (WOT) being representative of typical urban driving conditions, as in Table 2. Before each test, the engine was warmed up until the coolant and lubricating temperatures were stable at 80 and 90 °C, respectively. During the tests, the engine ran at a stoichiometric air-fuel ratio due to a feedback control on the injected fuel.

Table 2. Investigated conditions.

Fuel	Properties	Engine Speed [rpm]	IMEP [bar]
Gasoline	DI	2000	8.3
	DI	4000	8.7
	PFI	2000	8.9
	PFI	4000	9.8
E30	DI	2000	8.6
	DI	4000	8.7
	PFI	2000	8.6
	PFI	4000	9.6
Ethanol	DI	2000	8.9
	DI	4000	8.8
	PFI	2000	8.4
	PFI	4000	9.6

To keep the λ value constant, the duration of injection (DOI) was adjusted based on the equivalence ratio measured by the lambda sensor installed in the exhaust. The start of injection (SOI) and start of spark (SOS) were properly modified to maximize the maximum brake torque (MBT). Each measurement was repeated three times. In the following section, the average values of each test are shown; the variability among the measurements is around 5%.

2.3. Methodology

In order to evaluate the nature of sub-23 nm particles, it is important to better analyze the effect of the sampling conditions on the PSDs, thus, demonstrating the contribution of the volatile species in the size range 10–23 nm. For this reason, the measurements with the EEPS were done using the conditioning system in two different temperature setting conditions.

The first one, named HOT, is characterized by the temperature of the first diluter and of the evaporation chamber at 150 and 300 °C, respectively, as prescribed by the PMP protocol. In this case, the volatiles evaporate, and the measured particles can be considered solid even if artefacts in the conditioning unit might also occur. In the second condition, named COLD, the temperature of the first diluter and of the evaporation chamber are set at lower values, 30 and 50 °C, respectively, to promote condensation and nucleation phenomena. For the tests with the HM-DMA, the dilution temperature was fixed at 150 °C.

2.4. Tested Fuels

Tests were performed with commercial European gasoline, ethanol and a splash-blended 30% v/v ethanol in gasoline. The main physical–chemical properties of the pure fuels are listed in Table 3. The alcohol fuel presents properties associated with increased engine efficiency, such as easier evaporation, higher knock resistance and greater charge cooling. On other hand, it also poses the challenge of greater fuel consumption due to lower volumetric energy density [29].

Table 3. Fuel properties.

Properties	Gasoline	Ethanol
Density at 15 °C [kg/L]	0.751	0.790
Viscosity at 20 °C (mPa s)	0.39	1.19
LHV [MJ/L]	32.0	21.1
AFRst	14.7	9
Octane Number	98	108.6
Boiling point [°C]	27–225	78
Specific heat capacity [kJ/kgK]	2	2.4
C [% mass]	86.12	52.2
H [% mass]	13.25	13.1
O [% mass]	0.63	34.7
Aromatic content [% v/v]	35	-

3. Results and Discussion

Figures 3 and 4 show the PN measured for gasoline, E30 and ethanol fueling in DI and PFI configurations, respectively, at both 2000 and 4000 rpm. Measurements were performed with the EEPS coupled to the DEED working at the temperatures prescribed by the PMP protocol.

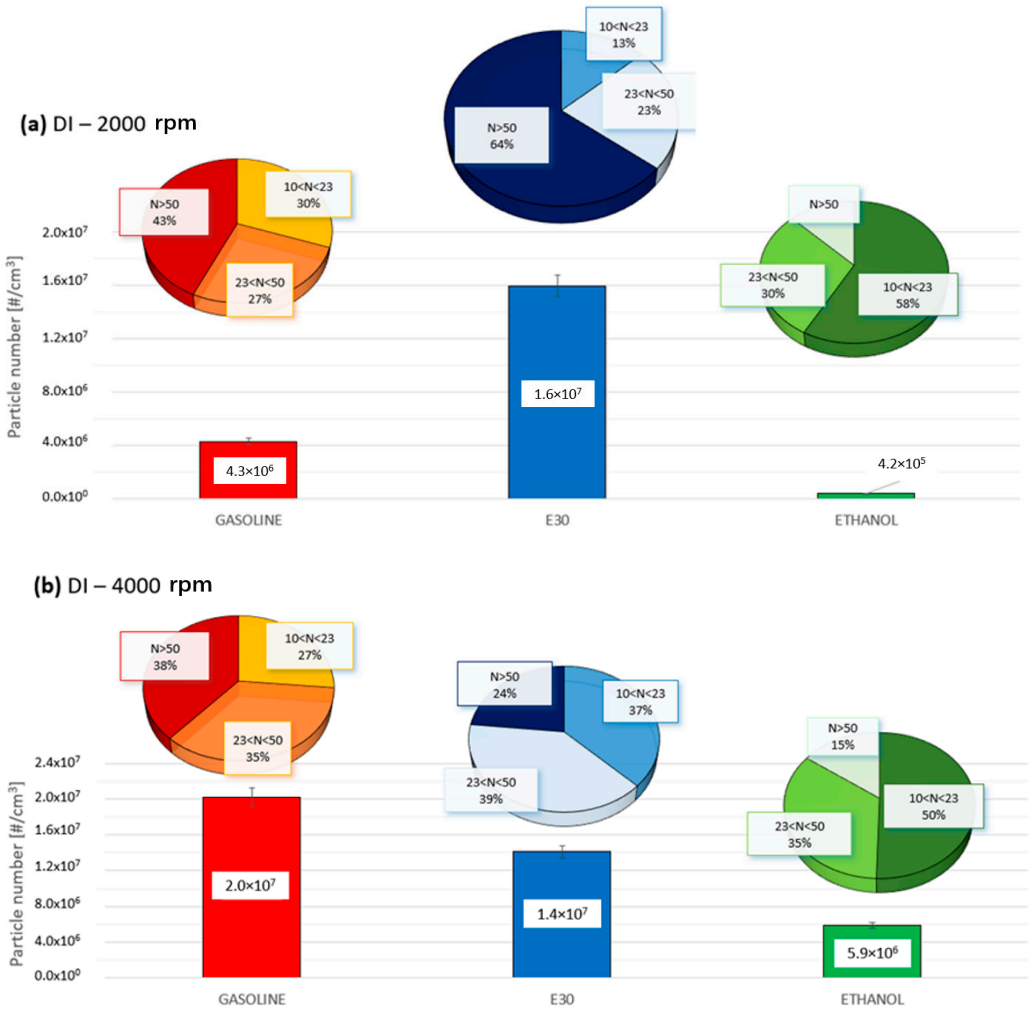

Figure 3. Particle number emitted in DI configuration for gasoline, E30 and ethanol fuels at (**a**) 2000 rpm and (**b**) 4000 rpm.

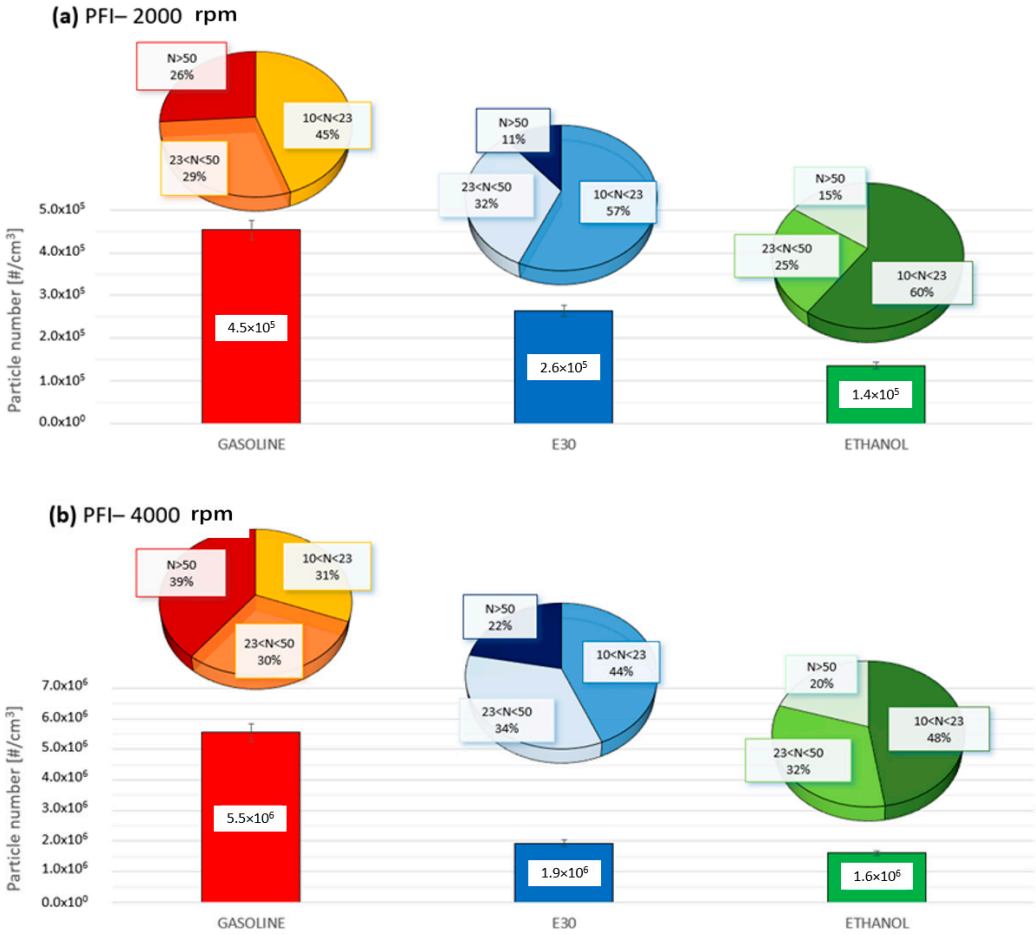

Figure 4. Particle number emitted in PFI configuration for gasoline, E30 and ethanol fuels at (**a**) 2000 rpm and (**b**) 4000 rpm.

The fraction of different dimensional range particles was calculated. In detail, three size ranges were selected: 10–23 nm particles, not included in the limit yet, and the particles larger than 23 nm, currently regulated, that are further divided in two classes, 23–50 nm as representative of the nuclei particles and particles larger than 50 nm typical of the accumulation particles. The particle concentration in the different ranges were calculated by integrating the particle size distributions between the two limits [30].

For all the operating conditions, it is possible to distinguish the three size classes particles even if their contribution change according to the engine configuration and operating condition as well as the fuel. Whatever the engine speed and fuel, the particle emission is larger for DI configuration (Figure 3) with respect to the PFI condition (Figure 4). The less time available for fuel evaporation and for air/fuel mixing as well as the large wall impingement are the main mechanisms of particle formation in DI engines [31]. On the other hand, in PFI configuration the fuel has more time for evaporation and mixing. In this case, the particles are formed in small rich zones localized across the valves where fuel does not evaporate completely and burns in a diffusive way, namely pool fire [32].

An important role is also played by the operating conditions. For both injection strategies, the general trend is an increase of PN at high engine speed. In the DI configuration, as the engine speed increases, the mixing time is shortened significantly, and the fuel impingement is further worsened because of the narrower gap between injector and piston typical of this operating condition, thus, resulting in a notable increase of PN. For PFI engine at 4000 rpm, the increase in the emission is ascribable to the larger pool flame across the intake valves due to the larger fuel supply.

The fuel effect on particle emissions changes according to the injection strategy and engine test point. In the DI configuration, at 2000 rpm (Figure 3a), we observed a decrease of PN for ethanol fueling compared to gasoline due to the physicochemical properties of the oxygenated fuel characterized by lower aromatic components that are considered as precursors of soot. On the other hand, the PN emitted by E30 is one order of magnitude higher with respect to gasoline fuel.

The reason is that the addition of ethanol to gasoline significantly impacts the shape of the distillation curve since the ethanol molecule forms an azeotrope with the hydrocarbon compounds, which can alter the liquid/vapor composition during the vaporization process. These interactions can retain the aromatic species within the liquid phase preventing their mixing, thus, promoting soot formation [33].

This phenomenon is accentuated at low speeds because of the low temperature that further worsens the evaporation. At high speeds, instead, a linear decrease of PN with the ethanol content is observed since, at higher temperature, the advantage provided by the biofuel properties on the soot formation is predominant. With regard to the size distribution, at low engine speeds, for gasoline fuel, the weight of nuclei particles is important even if it is limited to 57% by considering both the sub-23 and the 23–50 nm particles.

A lower contribution of particles smaller than 50 nm, 36% in total, is provided by ethanol blend since the atomization and evaporation deteriorate when the ethanol is added to gasoline at low percentage causing the formation of larger primary soot particles. On the other hand, the main contribution to the particles emitted from ethanol is given by nuclei particles that amount to 88%. The particles emitted from pure ethanol are smaller than those of gasoline due to the higher soot oxidation rate during the combustion and post-oxidation phases [34].

At high engine speed, in DI configuration for gasoline fueling, the sub-23 nm and the 23–50 nm particles count for 27% and 35%, respectively. In opposite trend with respect to the low speed condition, the weights of nuclei particles measured for the ethanol blend are higher than gasoline, 37% and 39% for the sub-23 nm and the 23–50 nm range, respectively. As mentioned, this trend can be ascribed to the higher temperature typical of the high engine speed that, together with the increased turbulence intensity, improve the mixing formation as ethanol is added to gasoline. A further increase of smaller particles is observed for pure ethanol characterized by 50% of 10–23 nm particles and 35% of particles in the range 23–50 nm.

Regarding the fuel effect on particle concentration and size distribution measured in PFI configuration (Figure 4), the beneficial effect of the lower propension to the soot formation characteristic of the alcohol fuel is dominant. The result is a decrease of PN as the ethanol content increases at both low and high engine speeds. The poor fuel vaporization that is the main cause of the higher PN measured for E30 in DI configuration at 2000 rpm is mitigated by the more time available for fuel vaporization and the absence of fuel impingement.

Moreover, the small amount of particles with less surface available to condense on results in more nuclei particles. The fraction of smaller particles, both the sub-23 nm and the 23–50 nm particles, increases for E30 and further for ethanol. In detail, the sub-23 nm particle percentage increases from 45%, 57%, up to 60% for gasoline, E30 and ethanol, respectively. Similarly, at 4000 rpm, the fraction of particles smaller than 23 nm is 31% for gasoline, 44% for E30 and 48% for pure ethanol.

It is well recognized that the measurement of particles is strongly sensitive to the dilution characteristics. Depending on the dilution ratio and temperature, semi-volatile organic species, mainly present in the sub-23 nm range, can adsorb and coagulate. Then, they nucleate and aggregate into large particles. These dynamic processes make the measurement of particles, and even more of those smaller than 23 nm, difficult.

In order to point out the effect of the sampling conditions, and particularly the temperature on the PSDs, measurements with the EEPS coupled to the DEED were performed in

two different temperature settings of the dilution system as described in the methodology section. For each distribution, the geometric mean diameter (*GMD*) was calculated [35] as

$$GMD = exp\left(\frac{\sum n_i ln d_i}{N}\right) \quad (1)$$

where d_i represents the characteristic particle diameter of the ith section, n_i is the PN concentration of the ith section, and N is the total PN concentration. The use of a geometric mean is preferable to using an arithmetic mean due to the logarithmic spacing of the size classes and the lower sensitivity to outliers. For a lognormal distribution, the *GMD* equals the median diameter. The effect of sampling temperature can be analyzed qualitatively through the observation of the PSDs. A quantitative metric based on the *GMD*, the Shift Ratio (*SR*), was defined for a more effective description. The SR was calculated as:

$$SR = \left(\frac{GMD_{COLD}}{GMD_{HOT}}\right) \quad (2)$$

so that *SR* values less than 1 reveal the propension to inception of nucleation mode particles, *SR* equal to 1 means that no significant shift is shown between the PSDs measured in both sampling configurations, *SR* greater than 1 is representative of the tendency to condensation onto existing particles. For a better comprehension of such phenomena, the PSDs measured for both *HOT* and *COLD* sampling conditions, in the three different cases identified by different values of *SR*, less, equal or greater than 1 are shown in Figure 5.

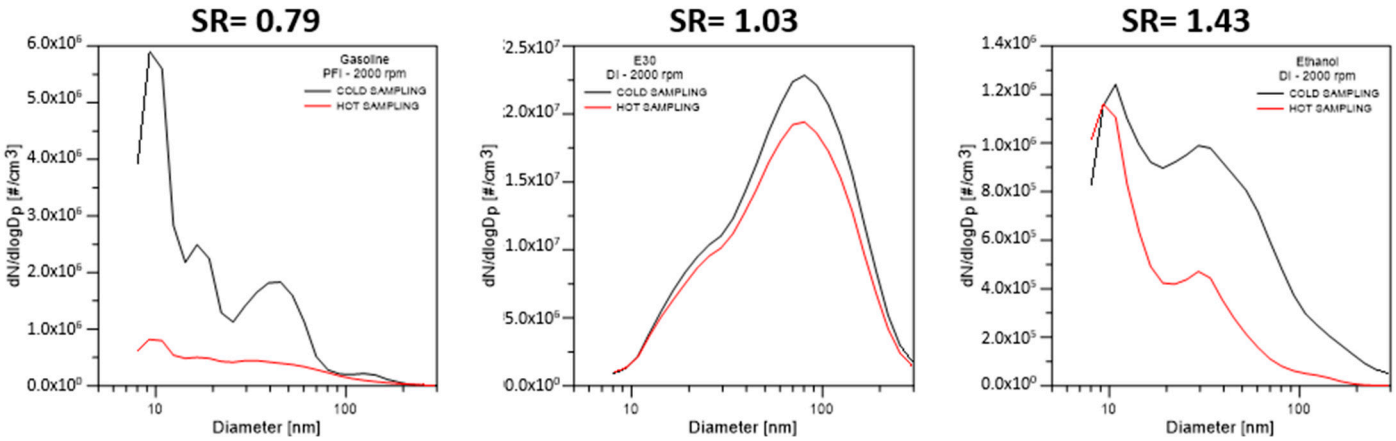

Figure 5. PSDs measured in both *COLD* and *HOT* sampling condition for three different *SR* values: 0.79, 1.03 and 1.43.

The first graph in which the *SR* is 0.79 refers to the PSDs measured in PFI configuration at 2000 rpm for gasoline fuel. Both distributions, in *COLD* and *HOT* sampling, are characterized by a bimodal shape with a first mode centered at 10 nm and a second mode peaking at 50 nm. The PSD measured at lower sampling temperature shows a larger particle number than that measured at higher temperature all over the size range, and it is more evident for the particles smaller than 30 nm. This behavior demonstrates that nucleation is the driving process. At low sampling temperature, the nucleation of volatiles is promoted resulting in the measure of a larger number of sub-23 particle compared to the condition at high temperature.

The second graph characterized by a *SR* of 1.03 shows the PSDs measured for E30 fueling in DI configuration at 2000 rpm. In this case, the different temperature settings do not significantly impact the PSD shapes. Lastly, the third graph is an example of PSDs characterized by a *SR* greater than 1.

They were measured in DI configuration at 2000 rpm for ethanol fueling. Both distributions exhibit a quite similar nucleation mode peaked at 10 nm and a second mode

centered at about 30 nm more pronounced for the sampling condition at lower temperature. In the *COLD* condition, the volatile components are mainly involved in the agglomeration process, thus, leading to the formation of larger agglomerates with respect to the *HOT* configuration.

Figure 6 summarizes the *SR* values obtained for the three tested fuels at all investigated conditions plotted versus the *GMD* of the PSDs measured in the *HOT* configuration. It arises that smaller particles are more likely to grow by condensation (*SR* > 1), and this trend is more evident for the ethanol blend and further for pure ethanol. Gasoline fuel, instead, especially in PFI configuration, mainly demonstrates a tendency to inception of nucleation mode particles. These results demonstrated the tendency of volatiles to nucleate or condense according to the number and the size of the particles.

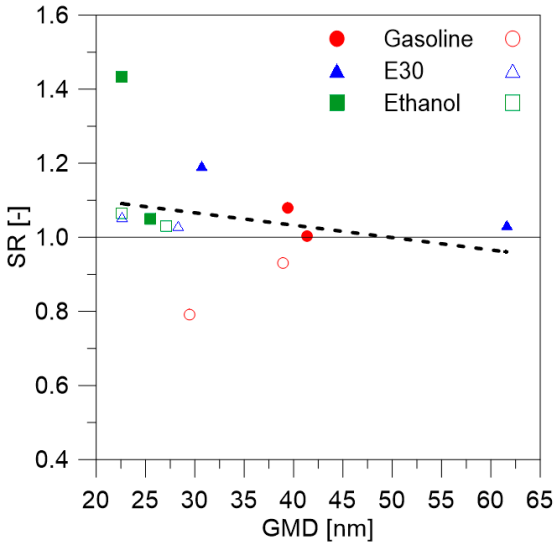

Figure 6. *SR* versus *GMD* for gasoline, E30 and ethanol at all investigated conditions in DI (full symbols) and PFI (empty symbols) configuration.

The results shown thus far have highlighted the impact of the sampling conditions on the particle emissions especially in the sub-23 nm range that will be subject to the next emission regulations, thus, indicating the need to define a proper procedure for the sampling and conditioning of the exhaust gas. As an innovative instrument, the advanced HM-DMA was designed to be capable of measuring particles in the range of 5–30 nm with a simplified conditioning unit. Figure 7 shows the ion concentration integrated in the range 10–23 nm measured for the tested fuels in both the DI and PFI layout.

In the DI configuration (Figure 7a) at 2000 rpm, in accordance with what was observed for the EEPS measurements, the ion concentration is reduced by one order of magnitude from gasoline, 3.2×10^6 #/cm^3 to pure ethanol fueling 2.1×10^5 #/cm^3. A significant increase, 8.9×10^6 #/cm^3, was instead observed for the ethanol blend. At high engine speeds, the ion concentration measured for gasoline and E30 reaches the same values, 1.7×10^7 #/cm^3 unlike the decreasing trend observed with the EEPS. Analogously to the measurement performed with the conventional system, a decrease of ion concentration down to 8.2×10^6 #/cm^3 was, instead, observed for ethanol.

In PFI configuration (Figure 7b), at 2000 rpm, it is not possible to discriminate a definite trend among the fuels since the measured ion concentrations are too low to be confused with the noise signal. On the other hand, at high engine speed, the ion concentrations measured for the tested fuels exhibit a different behavior than that detected with the experimental setup involving the EEPS.

The ion concentration measured with the advanced HM-DMA does not show a linear decreasing trend as the ethanol content increases. On contrary, the ion concentration increases from 2.6×10^5 #/cm^3 for gasoline up to 1.9×10^6 #/cm^3 for E30. A slightly

reduction was observed for pure ethanol even if the ion concentration is higher than that measured for gasoline. The different results obtained with the two different particle measurement systems is correlated to the different measurement principle. Moreover, an important role is also played by the sampling and conditioning system that is more simplified for the HM-DMA, thus, preventing particle losses due to diffusion and reducing the possibility that artefacts can occur in more complex sampling system, such as the re-nucleation phenomena that can occur in the evaporation tube of the conditioning system.

The correlation between the sub-23 nm particle concentration measures with the EEPS and the ion concentration obtained with the HM-DMA is synthetized in Figure 8 for all the tested fuels. A good correlation was found out for all tested fuels, $R^2 = 0.919$ for gasoline, $R^2 = 0.972$ for E30 and $R^2 = 0.996$ for ethanol.

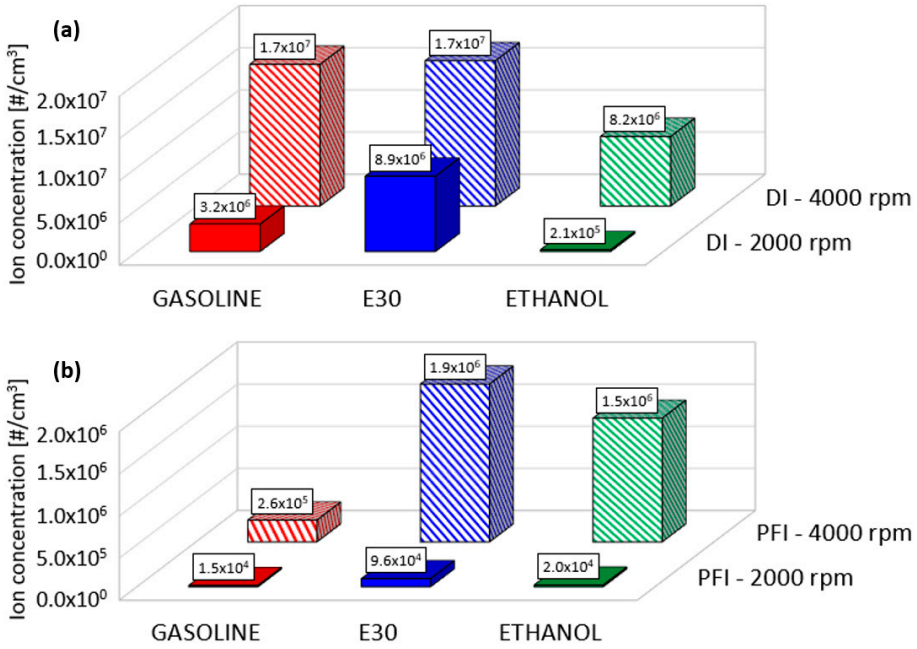

Figure 7. Ion concentration in the range 10–23 nm measured for gasoline, E30 and ethanol in (**a**) DI and (**b**) PFI configuration, both at 2000 and 4000 rpm.

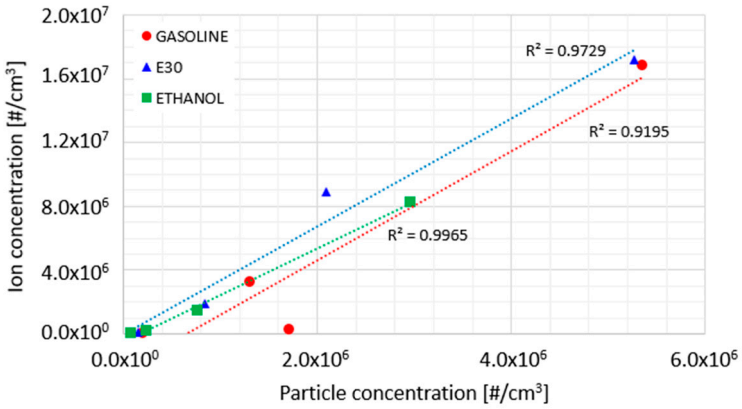

Figure 8. Ion concentration versus particle concentration in the range 10–23 nm for gasoline, E30 and ethanol at all investigated conditions.

4. Conclusions

This study was focused on the characterization of particle emissions at the exhaust of a SI engine equipped with both a PFI and a DI injection system through conventional and

novel instruments. Tests were done at different operating conditions by fueling the engine with gasoline and ethanol both pure and blended at 30% v/v.

Particles were measured by an EEPS coupled to the DEED, a conditioning system fulfilling the PMP protocol. To face the issues of artefacts that can occur in the sampling and dilution system, a novel aerosol measurement technology capable of operating at high temperatures, the advanced HM-DMA, was developed within the Sureal-23 project. It was coupled to a simplified sampling system consisting of a SD. We observed that a large portion of particles, whatever the operating condition and fuel, falls within the range 10–23 nm that is more prone to artifacts during the sampling.

For a quantitative analysis of the effect of sampling temperature on the particle emissions, a *SR* was calculated as the ratio of *GMD* of the PSDs measured at two different temperature settings. The tendency to inception of nuclei particles was distinguished for *SR* less than 1, while the inclination to condense on existing particles was observed for SR greater than 1. Measurements done with the advanced HM-DMA showed, in general, a good correlation with those performed through the EEPS. A disagreement between the two spectrometers was detected in PFI configuration at high engine speed due to the different measurement principle as well as the different sampling system.

This study highlighted the effect of sampling and measurement system on the measurement of sub-23 nm particles due to the presence of volatiles that can affect the final particle measures. This suggests the necessity of a specific measurement protocol considering the processes occurring during the sampling and conditioning.

Author Contributions: F.C., P.S. and S.D.I. curated the methodology and the investigation, A.M. and S.D.I. wrote the original draft, analyzed the findings and compiled the literature review. B.M.V. supervised and reviewed the entire study. All authors have read and agreed to the published version of the manuscript.

Funding: This work is part of Sureal-23 Project that has received funding from the European Union's Horizon 2020 research and innovation programme under grant agreement N. 724136.

Institutional Review Board Statement: Not applicable.

Informed Consent Statement: Not applicable.

Data Availability Statement: Data will be made available upon request.

Acknowledgments: Authors are thankful to the project partners E. Papaioannou, D. Zarvalis, P. Baltzopoulou, D. Zamora, Juan Carlos del Castillo, Rafael Delgado Ballesteros. The authors thank Carlo Rossi and Bruno Sgammato for the engine assessment and for the support in the experimental activity.

Conflicts of Interest: The authors declare no conflict of interest.

Abbreviations

AFR_{st}	Stoichiometric Air/Fuel ratio
CI	Compression Ignition
CPC	Condensation Particle Counter
DEED	Dekati® Engine Exhaust Diluter
d_i	particle diameter of *i*th section
DI	Direct Injection
DOI	Duration of Injection
DPF	Diesel Particulate Filter
EEPS	Engine Exhaust Particle Sizer Spectrometer
ET	Evaporation Tube
E30	30% *v/v* of Ethanol in gasoline blend
GMD	Geometric Mean Diameter

HM-DMA	Half Mini Differential Mobility Analyser
ICE	Internal Combustion Engine
LHV	Low Heating Value
λ	Excess air ratio
MBT	Maximum Brake Torque
N	Total Particle Number
n_i	particle concentration of *i*th section
PECU	Programmable Electronic Control Unit
PFI	Port Fuel Injection
p_{inj}	Injection pressure
PMP	Particulate Measurement Programme
PN	Particle Number
PSD	Particle Size Distribution
SD	Single Diluter
SEADM	Sociedad Europea de Analisis Diferencial de Movilidad
SESI	Secondary ElectroSpray Ionization
SI	Spark Ignition
SOI	Start of Injection
SOS	Start of Spark
SR	Shift Ratio
WOT	Wide Open Throttle

References

1. Turner, J.W.G.; Lewis, A.G.J.; Akehurst, S.; Brace, C.J.; Verhelst, S.; Vancoillie, J.; Sileghem, L.; Leach, F.; Edwards, P.P. Alcohol fuels for spark-ignition engines: Performance, efficiency and emission effects at mid to high blend rates for binary mixtures and pure components. *Energies* **2020**, *13*, 6390. [CrossRef]
2. Reitz, R.D.; Ogawa, H.; Payri, R.; Fansler, T.; Kokjohn, S.; Moriyoshi, Y.; Agarwal, A.K.; Arcoumanis, D.; Assanis, D.; Bae, C.; et al. IJER editorial: The future of the internal combustion engine. *Int. J. Engine Res.* **2020**, *21*, 3–10. [CrossRef]
3. Raza, M.; Chen, L.; Leach, F.; Ding, S. A Review of particulate number (PN) emissions from gasoline direct injection (gdi) engines and their control techniques. *Energies* **2018**, *11*, 1417. [CrossRef]
4. Kontses, A.; Triantafyllopoulos, G.; Ntziachristos, L.; Samaras, Z. Particle number (PN) emissions from gasoline, diesel, LPG, CNG and hybrid-electric light-duty vehicles under real-world driving conditions. *Atmos. Environ.* **2020**, *222*, 117126. [CrossRef]
5. Awad, O.I.; Mamat, R.; Ibrahim, T.K.; Hammid, A.T.; Yusri, I.M.; Hamidi, M.A.; Humada, A.M.; Yusop, A.F. Overview of the oxygenated fuels in spark ignition engine: Environmental and performance. *Renew. Sustain. Energy Rev.* **2018**, *91*, 394–408. [CrossRef]
6. Bokor, C.; Rohani, B.; Humphries, C.; Morrey, D.; Bonatesta, F. Investigating the impact of gasoline composition on PN in GDI engines using an improved measurement method. *Int. J. Engine Res.* **2021**, *22*, 3391–3406. [CrossRef]
7. Liu, H.; Li, Z.; Xu, H.; Ma, X.; Shuai, S. Nucleation mode particle evolution in a gasoline direct injection engine with/without a three-way catalyst converter. *Appl. Energy* **2020**, *259*, 114511. [CrossRef]
8. Di Iorio, S.; Catapano, F.; Sementa, P.; Vaglieco, B.M.; Nicol, G.; Sgroi, M.F. *Sub-23 nm Particle Emissions from Gasoline Direct Injection Vehicles and Engines: Sampling and Measure*; SAE Technical Paper; SAE International: Warrendale, PA, USA, 2020. [CrossRef]
9. Di Iorio, S.; Catapano, F.; Magno, A.; Sementa, P.; Vaglieco, B.M. Investigation on sub-23 nm particles and their volatile organic fraction (VOF) in PFI/DI spark ignition engine fueled with gasoline, ethanol and a 30 %v/v ethanol blend. *J. Aerosol Sci.* **2021**, *153*, 105723. [CrossRef]
10. Giechaskiel, B.; Manfredi, U.; Martini, G. Engine Exhaust Solid Sub-23 nm Particles: I. Literature Survey. *SAE Int. J. Fuels Lubr.* **2014**, *7*, 950–964. [CrossRef]
11. Giechaskiel, B.; Martini, G. Engine Exhaust Solid Sub-23 nm Particles: II. Feasibility Study for Particle Number Measurement Systems. *SAE Int. J. Fuels Lubr.* **2014**, *7*, 935–949. [CrossRef]
12. Andersson, J.; Mamakos, A.; Giechaskiel, B.; Carriero, M.; Martini, G. Particle Measurement Programme (PMP) Heavy-Duty Inter-laboratory Correlation Exercise (ILCE_HD) Final Report. 2010. Available online: https://op.europa.eu/en/publication-detail/-/publication/d095737d-d442-4dfb-a557-da1ef6308125/language-en (accessed on 4 March 2022).
13. Giechaskiel, B.; Melas, A.D.; Lähde, T.; Martini, G. Non-Volatile Particle Number Emission Measurements with Catalytic Strippers: A Review. *Vehicles* **2020**, *2*, 342–364. [CrossRef]
14. Zheng, Z.; Durbin, T.D.; Karavalakis, G.; Johnson, K.C.; Chaudhary, A.; Cocker, D.R.; Herner, J.D.; Robertson, W.H.; Huai, T.; Ayala, A.; et al. Nature of sub-23-nm particles downstream of the European particle measurement programme (PMP)-compliant system: A real-time data perspective. *Aerosol Sci. Technol.* **2012**, *46*, 886–896. [CrossRef]
15. Zheng, Z.; Johnson, K.C.; Liu, Z.; Durbin, T.D.; Hu, S.; Huai, T.; Kittelson, D.B.; Jung, H.S. Investigation of solid particle number measurement: Existence and nature of sub-23nm particles under PMP methodology. *J. Aerosol Sci.* **2011**, *42*, 883–897. [CrossRef]

16. Alföldy, B.; Giechaskiel, B.; Hofmann, W.; Drossinos, Y. Size-distribution dependent lung deposition of diesel exhaust particles. *J. Aerosol Sci.* **2009**, *40*, 652–663. [CrossRef]
17. Oberdürster, G. Toxicology of ultrafine particles: In vivo studies. *Philos. Trans. R. Soc. Lond. Ser. A Math. Phys. Eng. Sci.* **2000**, *358*, 2719–2740. [CrossRef]
18. Barrios-Collado, C.; Melas, A.; Baltzopoulou, P.; Vlachos, N.; Zarvalis, D.; Chasapidis, L.; Deloglou, D.; Daskalos, E.; Papaioannou, E. Understanding, Measuring and Regulating Sub-23 nm Particle Emissions from Direct Injection Engines Including Real Driving Conditions. Project:SUREAL-23. Project Number: 724136. 2017. Available online: https://wiki.unece.org/download/attachments/58525453/PMP-47-11%20SUREAL23_PMP_47.pdf?api=v2 (accessed on 4 March 2022).
19. Catapano, F.; Di Iorio, S.; Magno, A.; Vaglieco, B.M. Effect of fuel quality on combustion evolution and particle emissions from PFI and GDI engines fueled with gasoline, ethanol and blend, with focus on 10–23 nm particles. *Energy* **2022**, *239*, 122198. [CrossRef]
20. Fernández de la Mora, J.; Kozlowski, J. Hand-held differential mobility analyzers of high resolution for 1-30nm particles: Design and fabrication considerations. *J. Aerosol Sci.* **2013**, *57*, 45–53. [CrossRef]
21. Differential Mobility Analysis | SEADM. Available online: https://www.seadm.com/differential-mobility-analysis/ (accessed on 21 November 2021).
22. Zinola, S.; Leblanc, M.; Rouleau, L.; Dunand, X.; Baltzopoulou, P.; Chasapidis, L.; Deloglou, D.; Melas, A.D.; Konstandopoulos, A.G.; Rüggeberg, T.; et al. *Measurement of Sub-23 nm Particles Emitted by Gasoline Direct Injection Engine with New Advanced Instrumentation*; SAE Technical Paper; SAE International: Warrendale, PA, USA, 2019. [CrossRef]
23. TSI. Updated Inversion Matrices for Engine Exhaust Particle SizerTM (EepsTM) Spectrometer Model 3090—Application Note EEPS-005 (A4). Volume 5. Available online: https://tsi.com/getmedia/22bf0106-13d9-4503-b179-bc76cb55e100/Updated_Inversion_Matrices_EEPS-005-A4-web?ext=.pdf (accessed on 4 March 2022).
24. Wang, X.; Grose, M.A.; Avenido, A.; Stolzenburg, M.R.; Caldow, R.; Osmondson, B.L.; Chow, J.C.; Watson, J.G. Improvement of Engine Exhaust Particle Sizer (EEPS) size distribution measurement—I. Algorithm and applications to compact-shape particles. *J. Aerosol Sci.* **2016**, *92*, 95–108. [CrossRef]
25. Fernandez de la Mora, J. Expanded flow rate range of high-resolution nanoDMAs via improved sample flow injection at the aerosol inlet slit. *J. Aerosol Sci.* **2017**, *113*, 265–275. [CrossRef]
26. Fernandez de la Mora, J.; Perez-Lorenzo, L.J.; Arranz, G.; Amo-Gonzalez, M.; Burtscher, H. Fast high-resolution nanoDMA measurements with a 25 ms response time electrometer. *Aerosol Sci. Technol.* **2017**, *51*, 724–734. [CrossRef]
27. Baltzopoulou, P.; Melas, A.D.; Vlachos, N.; Deloglou, D.; Papaioannou, E.; Konstandopoulos, A.G. *Solid Nucleation Mode Engine Exhaust Particles Detection at High Temperatures with an Advanced Half Mini DMA*; SAE Technical Paper; SAE International: Warrendale, PA, USA, 2020; Volume 1, pp. 535–542. [CrossRef]
28. Amo, M.; Barrios, C.; Castillo, J.C.; De Mora, J.F.; Konstandopoulos, A.G. Half-mini DMA modification for high temperature aerosols and evaluation on various combustion exhausts. In Proceedings of the European Aerosol Conference, Zurich, Switzerland, 28 August–1 September 2017.
29. Larsson, T.; Stenlaas, O.; Erlandsson, A. *Future Fuels for DISI Engines: A Review on Oxygenated, Liquid Biofuels*; SAE Technical Paper; SAE International: Warrendale, PA, USA, 2019; Volume 2019, pp. 1–23. [CrossRef]
30. TSI. *Incorporated Engine Exhaust Particle SizerTM Spectrometer Model 3090*; TSI Inc.: Shoreview, MN, USA, 2016; p. 8. Available online: https://tsi.com/products/particle-sizers/fast-particle-sizer-spectrometers/engine-exhaust-particle-sizer-(eeps)-3090/ (accessed on 4 March 2022).
31. Awad, O.I.; Ma, X.; Kamil, M.; Ali, O.M.; Zhang, Z.; Shuai, S. Particulate emissions from gasoline direct injection engines: A review of how current emission regulations are being met by automobile manufacturers. *Sci. Total Environ.* **2020**, *718*, 137302. [CrossRef] [PubMed]
32. Catapano, F.; Di Iorio, S.; Sementa, P.; Vaglieco, B.M. *Characterization of Ethanol-Gasoline Blends Combustion Processes and Particle Emissions in a GDI/PFI Small Engine*; SAE Technical Paper; SAE International: Warrendale, PA, USA, 2014; Volume 1, p. 1382. [CrossRef]
33. Burke, S.; Rhoads, R.; Ratcliff, M.; McCormick, R.; Windom, B. *Measured and Predicted Vapor Liquid Equilibrium of Ethanol-Gasoline Fuels with Insight on the Influence of Azeotrope Interactions on Aromatic Species Enrichment and Particulate Matter Formation in Spark Ignition Engines*; SAE Technical Paper; SAE International: Warrendale, PA, USA, 2018; pp. 10–12. [CrossRef]
34. Myung, C.L.; Choi, K.; Cho, J.; Kim, K.; Baek, S.; Lim, Y.; Park, S. Evaluation of regulated, particulate, and BTEX emissions inventories from a gasoline direct injection passenger car with various ethanol blended fuels under urban and rural driving cycles in Korea. *Fuel* **2020**, *262*, 116406. [CrossRef]
35. Eastwood, P. *Particulate Emissions from Vehicles*; John Wiley & Sons: Hoboken, NJ, USA, 2008. [CrossRef]